

p-Phenylenediamine electrochemical oxidation revisited: an insight into the mechanism and kinetics in acid medium

Ángela Fernandez-Merino, Rafael del Caño, Miriam Chávez, Guadalupe Sánchez-Obrero, Rafael Madueño, Manuel Blázquez, Teresa Pineda

Departamento de Química Física y Termodinámica Aplicada; Instituto Químico para la Energía y el Medio Ambiente.
Universidad de Córdoba, 14071 - Córdoba

Abstract

The present study is focused on the electrochemical oxidation of p-phenylenediamine in aqueous acid solution. A general view of the process in a wider pH range is first presented to highlight the unique features taking place in the acid medium. The oxidation process in this pH range involves two electrons and three or two protons to yield the diimine quinone species. A quasi-reversible electron transfer with rate constants of 6×10^{-4} and 6.4×10^{-4} cm/s are determined by cyclic voltammetry and rotating disk voltammetry, respectively. The presence of a second reduction peak that is strongly dependent on the scan rate and the solution pH indicates the occurrence of a chemical reaction in which the oxidation product is involved. The analysis of the cyclic voltammetric curves indicates that the subsequent chemical reaction generates an electroactive species that can be reduced within the potential range of the voltammetric scan. Controlled potential electrolysis allows us to determine the characteristics of the oxidation process as well as the nature of the chemical reaction. A diimine quinone hydrolysis reaction involving both imine groups, accounting for the 60% conversion to benzoquinone, together with the reaction of the parent diamine with the diimine quinone product to yield the semiquinone free radical are proposed to take place immediately after the oxidation reaction. The presence of other coupling reaction yielding dimer or trimer species such as the Brandowski's base cannot be discarded.

1. Introduction

For many years, p-phenylenediamine (pPD) derivatives have been used as precursors in oxidation reactions for permanent hair dye formulations, besides they have been qualified as potent contact allergens and carcinogenic by the expert panel's Cosmetic Ingredient Review (CIR) [1]. In this sense, electrochemical oxidation reactions, either homogeneous or heterogeneous, have been the object of early studies that attempted to clarify the reaction paths as well as the final oxidation products [2-10]. However, systematic studies dealing with the heterogeneous electrochemical mechanisms in aqueous solutions have not been reported.

On the other hand, the development of carbon nanomaterials with luminescent properties has been the subject of research in recent years, highlighting among them multicolored carbon dots (MCDs) [11]. These are small carbon nanoparticles that have emission properties in different regions of the spectrum, which makes them potentially applicable in various fields such as electronics or health. Among the most used precursors in the synthesis of MCDs are the phenylenediamine isomers and much literature has been generated related to the

compounds that can be formed and that would be at the origin of the fluorescence, especially that produced in the red region [12]. In this sense, a study of the oxidation of pPD in aqueous solutions is of the most interest in order to clarify some of the reactions that occur between the oxidized species that are generated in that synthesis processes, as well as between them and the precursor molecule itself.

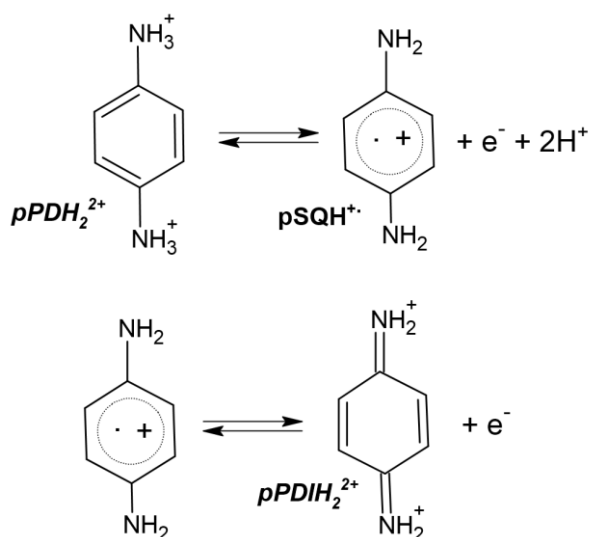
Several research groups have studied the oxidation of pPD derivatives [13-17] that should behave in a similar way that the pPD parent, although no systematic studies have been reported on the latter compound. By using thin-layer electrochemistry, Plichon et al. [13] studied the oxidation of N,N-dimethyl-p-phenylenediamine in acid and neutral aqueous solutions and found a two-electron oxidation path taking place in two separate steps a $\text{pH} > 4$. They also tried to evaluate the coupled chemical reaction, but they found it too slow to be measured by this approximation. However, at lower pH, the oxidation of the intermediate product was facilitated by the disappearance of the final product by a chemical reaction that was ascribed to the hydrolysis of the quinone diimine final product giving place to the quinone monoimine species. In neutral media, the behavior completely changes. It seems that the hydrolysis is now substituted by a dimerization reaction. The controlled potential electrolysis of N,N-dimethyl-p-phenylenediamine at pH 2.2 involves 3 electrons per mol of reactive and the solution changes from almost transparent to an intense violet color typical of Wurster red radical cation, within the first minutes, that soon disappears. Moreover, the occurrence of a 1,4-addition reaction between the parent molecule and the quinone monoimine species was also described to explain the involvement of 3 electrons in the overall reaction [14].

The complexity of the overall oxidation pathway of N,N-dimethyl-p-phenylenediamine was evidenced by studies of the final products obtained by using an on-line electrochemical-mass spectrometry approach that allows to determine the evolution of the products with the time they spent in the reactor chamber [16]. Under these conditions, the system was able to detect different homogeneous post-reactions that can help in the elucidation of the behavior under different pH in aqueous solutions. Thus, formation of Wurster red cation radical, quinone diimine and monoimine as well as dimer and trimer products from coupling reactions of the different existing species occur which concentration were dependent on the pH reaction medium.

In a study conducted at pH 7 by using a rotating disk electrode [15], N,N-dimethyl-p-phenylenediamine showed limiting currents, consistent with a two-electrons oxidation, that follow the Levich equation allowing the determination of the diffusion coefficient, that is very

similar to the obtained by the micro-disk experiments. In a study using sonovoltammetry, the two-electron global signal is split, because of the diffusional overpotential that affect the second electron transfer that get slower than the first one and moves to higher potentials. When the study is carried out in organic solvents under hydrodynamic conditions and conventional cyclic voltammetry [18, 19], two well defined signals appear that indicate that the oxidation behaves as a reversible one-electron charge transfer reaction that can be complicated by chemical reactions followed by a second charge transfer, postulating an ECE mechanism for the first wave. This wave can also be theoretically simulated to an $EC_{rev}ECE$ mechanism, suggesting that the second oxidation wave could be due to the oxidation of an addition product formed between the parent compound and de diimine species. However, in a recent work [17], the correlation of the voltammetric results with the EPR studies that evidence that the radical cation is the major product after the first voltammetric wave, point to the fact that the radical cation is not the first oxidation product, but there is a time lag in its appearance in solution after the first step. They speculate with the formation of a mixed valent dimer that adsorbs on the electrode surface, formed by proton transfer and H-bonding between the adsorbed radical cations, that once desorbed is converted into the monomers. Thus, the gradual breakup of the dimer in solution leads to the appearance of the second wave.

In an attempt to demonstrate the presence of the semiquinone free radical ($pSQH^{\cdot+}$) as an intermediate in the oxidation pathway of pPD, the oxidation of this molecule was carried out in 50% methanol/water mixtures in acid medium (Scheme 1) [20].



Scheme 1. Oxidation pathway of pPD in 50% methanol/water mixtures in acid medium.

Although an electron spin resonance spectrum similar to that found in aqueous solutions was obtained [6], the amount of the $pSQH^{\cdot+}$ free radical was much smaller than that of $pPDIH_2^{2+}$

species. Finally, the conversion of the pPDH_2^{2+} to benzoquinone by hydrolysis is proposed [20]. At neutral pH, the RDE behavior of pPD allows the determination of the diffusion coefficient of $6.6 \times 10^{-6} \text{ cm}^2/\text{s}$ [21] assuming the transfer of two electron in the oxidation reaction. Under these conditions, a subsequent 1,4-addition reaction involving the pPDH_2^{2+} and the parent molecule is proposed.

The use of room temperature ionic liquids (RTILs) in electrochemistry provides an ideal medium to work in the absence of water. Under these conditions, several pPD derivatives have been studied by using microelectrode voltammetry showing that two well separated one-electron peaks are obtained corresponding to the transformation into the free radical cation and the subsequent dication. This fact allows for the determination of the rate constants of every charge transfer reaction and the diffusion coefficients of the three species. The higher viscosity of the RTIL environment provoke the diffusion coefficients of the involved species to be different, something that is not normally taken in account in aqueous or organic solvents [22-25].

In this work, we study the oxidation of pPD in aqueous solutions by means of different electrochemical techniques such as cyclic voltammetry (CV), differential pulse voltammetry (DPV), chronoamperometry (CA) and, rotating disc electrode voltammetry (RDE). After a general view of the process in a wide range of pHs, a deeper study is presented in acidic conditions. A two-electron oxidation mechanism for pPD in acid medium is found that should give the corresponding quinone diimine. After exhaustive electrolysis at controlled potential, benzoquinone is found as a major final product evidencing the fast hydrolysis reaction of the two imine groups of the quinone diimine, under these conditions.

2. Experimental section

2.1. Reactants

p-phenylenediamine (pPD), benzoquinone (BQ) and 4-aminophenol (AP) were obtained from Sigma-Aldrich. The rest of reagents were from Merck analytical grade. All the solutions were prepared with deionized water ($18.2 \text{ M}\Omega/\text{cm}$). The working solutions were prepared with either Britton – Robinson buffer at different pH or HCl and H_2SO_4 at different concentrations and were purged with N_2 gas for 30 min to maintain a negligible level of dissolved O_2 , and a continuous N_2 gas flow was positioned above the solution to prevent the ingress of O_2 during the electrochemical experiments.

2.2. Apparatus and methodology

Electrochemical experiments were conducted in an Autolab PGSTAT 30. For cyclic voltammetry (CV), differential pulse voltammetry (DPV) and chronoamperometry (CA), the working electrode was a glassy carbon (GC) disk (3 mm diameter) from I.J. Cambria LTD. Rotating disc experiments were carried out with a GC electrode (3 mm diameter) from Taccusel with an analytical rotator speed controller. Reference Ag/AgCl (3M KCl) and platinum counter electrode were from Metrohm. The GC electrodes were polished using alumina slurry and submitted to an ultrasound bath, before every experiment. The working electrode used in electrolysis was a reticulated vitreous carbon electrode of a high surface area from Bioanalytical Systems Inc. This electrode was cleaned by immersing it in piranha solution and submitted to an ultrasound bath to remove all the adsorbed substances.

The DPVs were recorded by using a step potential of 5 mV and a modulation time of 0.05 s at an interval time of 0.5 s. These parameters allowed a scan rate of 10 mV/s. CA curves were measured by equilibrating the system at the initial potential and stepping to a final value where the signal was recorded. The monitored time was higher than 10 s. To investigate the electrochemical process and the nature of the final oxidation products, a controlled potential electrolysis has been carried out. The charge was monitored by chronocoulometry. A 5 mM pPD solution in Britton-Robinson buffer at pH 1.8 was placed in the electrochemical cell and, after removing the oxygen, the potential was set at 1 V. Aliquots of the electrolysis mixture were taken at different time or charge values and diluted in the same buffer up to reach 1 mM concentration. Cyclic voltammograms and UV-visible spectra were recorded to follow the process. The cyclic voltammograms were recorded by using the GC electrode of 3 mm diameter to compare the results with the rest of experiments carried out.

Likewise, these solutions have been monitored by absorption spectroscopy using cells with two optical pathlengths, in order to obtain appropriate signals in both the UV and visible regions, as the visible bands are much weaker. UV-visible absorption spectra were recorded in a Jasco V-670 UV-vis-NIR spectrophotometer. Quartz cells of 0.2 and 1 cm pathlength were used.

3. Results and discussion

3.1. General behavior. Cyclic voltammetry of pPD in aqueous solutions

The electrochemical oxidation process of pPD in aqueous solution (Britton-Robinson buffer 0.1 M) seems very simple at a first glance. We have carried out a study by cyclic voltammetry in a wide pH range by using 1 mM pPD, a concentration that presumably does not favor polymerization reactions [26-31]. An anodic peak (O1) is observed by cyclic voltammetry

in a wide pH range and one or two reduction peaks (R1 and R2) upon reversing the potential scans which occurrence is only observed in acid medium (Figure 1). The peak potentials, E_p , show a variation with pH as shown in Figure 2 where three regions (I, II and III) can be distinguished with slopes for the direct scans that are similar to those obtained from the parameters measured in the reverse scans (Table 1). Although the slopes ($\partial E_p / \partial \text{pH}$) obtained in regions II and III are analogous, they define two regions where the irreversibility of the process changes, being more irreversible in region III, where a sudden increase in the peak potential separation is clearly observed. As it is shown in Figure 2b, the values for the oxidation and reduction peak separations, ΔE , change from 100 mV at $\text{pH} < 4$, decreases to 60 mV and finally gets a value much higher than 200 mV. Two inflections are observed in this curve at pH around 4 and 8.3 that fairly coincide with the changes in the $\partial E_p / \partial \text{pH}$ values.

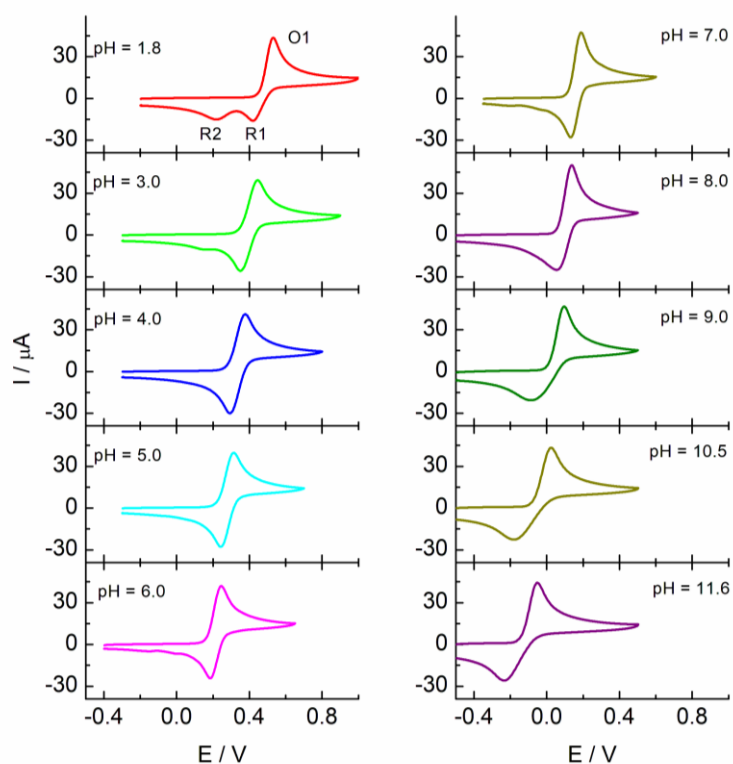


Figure 1. Cyclic voltammograms of pPD with a GC electrode at different pHs. (pPD) = 1 mM in Britton-Robinson buffer 0.1 M. Scan rate is 0.1 V/s.

Table 1. Experimental variations of E_p with pH for the direct (Ox) and reverse (Red) scans for the redox process of pPD in aqueous solution.

Region	pH interval	$\partial E_p / \partial \text{pH}$ (Ox)	$\partial E_p / \partial \text{pH}$ (Red)
I	< 2.5	-82.4	-78.6
II	2.5 < pH < 8.5	-63.2	-55.6
III	> 8.5	-64.8	-59.5

The peak currents for the oxidation process vary with pH, with a higher value at pH ~ 8, showing some parallelism with the three mentioned pH regions (Figure 2c). The reduction currents are lower than the oxidation ones being this in a ratio from 1 to 1.5, as shown in Figure 2d. Moreover, the ratio in acid medium reaches a value of 2, probably due to the influence of the second reduction peak obtained under these conditions that should compete with the main peak R1. These features point to the existence of a fast chemical reaction subsequently to the main oxidation process.

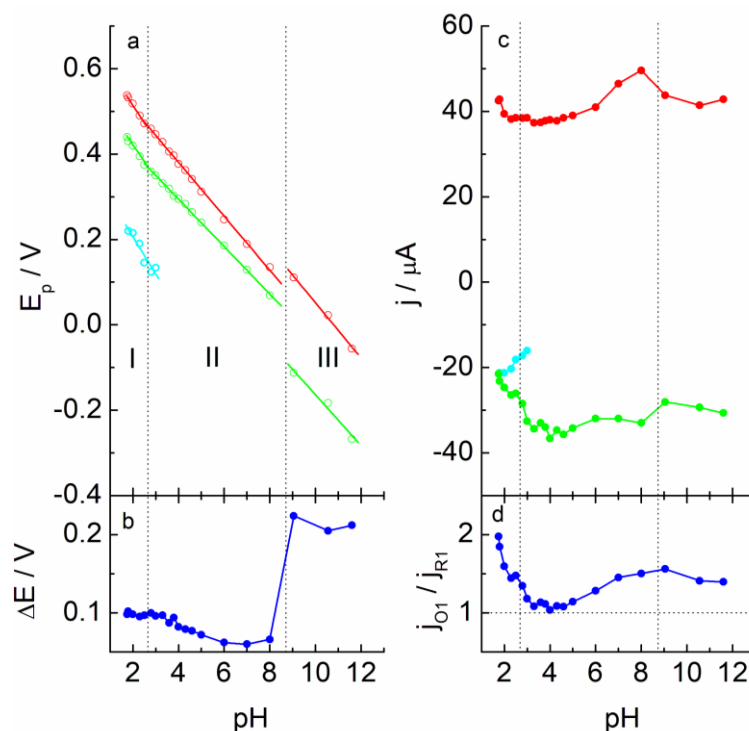
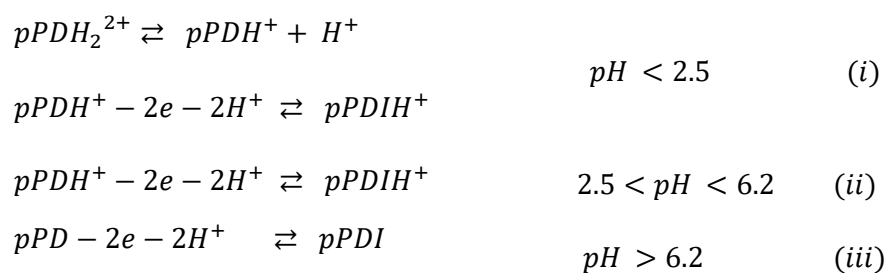
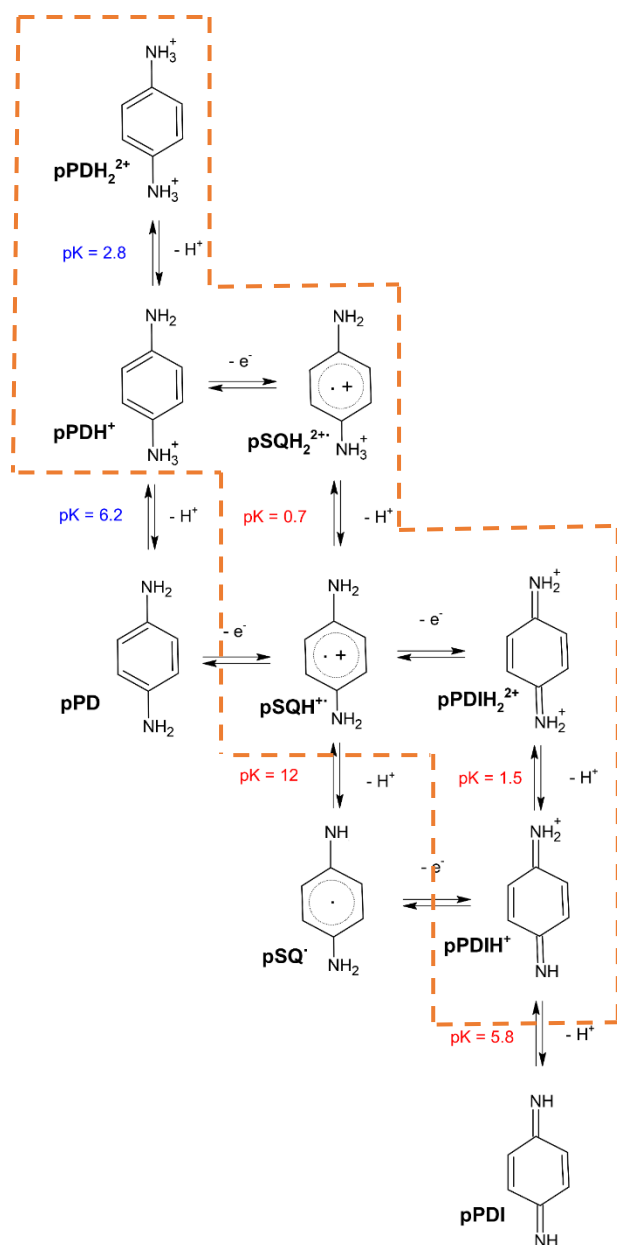


Figure 2. Variation of the peak potential, E_p (a), peak potential difference, ΔE (b), peak current density, j (c) and, anodic to cathodic current ratio j_{O1}/j_{R1} (d) as a function of pH, determined from the cyclic voltammograms of Figure 1. — O1; — R1; — R2.

The behavior of pPD in aqueous solutions is then strongly related with the acid-base equilibrium of this molecule. It is known that pPD has pK values of 2.8 and 6.2, as determined by UV-visible absorption spectroscopy (Figure S1, Scheme 2) [5, 17, 32]. Thus, at lower pHs, the species in solution is the diprotonated one (pPDH_2^{2+}) which, after losing a proton becomes monoprotated (pPDH^+), which must be the electroactive species. This is deduced from the somewhat higher variation of the peak potentials at $\text{pH} < 2.5$. From this pH value, the variation is the same throughout the studied range, indicating that the same number of protons and electrons is involved in the oxidation process, according to the Nernst equation. Hence, the general oxidation mechanism for pPD can be proposed as:



This reaction scheme agrees with the results obtained so far in the CV study. In acid medium, the diprotonated $pPDH_2^{2+}$ must lose a proton to get the electroactive species ($pPDH^+$), and at $pH > 2.5$, the solution species, $pPDH^+$, is directly oxidized to get the diimine species. At pH higher than the second pK (c.a. $pH > 6.2$) the electroactive species change to the neutral pPD , producing an increase in the irreversibility of the system as seen by the increase in peak separation observed that give place to region III (Figure 2). This fact would be related with the absence of charge in the neutral pPD .



Scheme 2. Aqueous solution species in all the pH range [17]. The box drawn in an orange broken line encloses the proposed path followed by the oxidation of pPD in an acid medium, as discussed through the text.

In what follow in this work, we will focus on the behavior of the pPD oxidation in the region of acid pH. In an incoming paper, we will report on the different mechanisms taking place at either neutral or alkaline pHs.

3.2. Electrochemical process in acid medium

3.2.1. Differential pulse voltammetry study (DPV)

With the aim of investigating the origin of the two reduction peaks observed in acid medium, a DPV study in this pH region has been carried out (Figure 3). The DPV curves show a main oxidation peak and two reduction peaks with characteristics similar to those found in CV. As this technique is more sensitive to the detection of processes [33], together with the lower scan rate used, it has been possible to detect the presence of other oxidation and reduction peaks of a much lower intensity. The variation of the peak potentials with pH is also shown in Figure 3. These additional peaks are found in the region of higher potentials than the main peak and must be related to collateral redox processes that take place due to the great reactivity of the intermediates and/or reaction products that originate in the electrochemical process. However, even at the low scan rate with which these DPV curves are recorded, peaks O1''/R1'' and O1'/R1' are imperceptible in the ordinary scale and need to be enlarged (more than 10-fold) to be observed (see insert in Figure 3a), which would indicate that these reactions are very slow and should not influence the main redox process of pPD that we are studying.

Continuing the analysis with the description of the behavior of peaks O1, R1 and R2, which correspond to the main peaks obtained by CV, it should be noted that the variation of the potential of peaks O1/R1 shows slopes somewhat lower than that observed in CV (Tables 1 and 2), and which has been ascribed to the loss of an H⁺ ion to give rise to the electroactive species pPDH⁺. Therefore, the DPV results would agree with the involvement of only 2 H⁺ in the overall reaction in this pH range. It is interesting to highlight the virtually zero separation of the anodic and cathodic peaks, which would be related to a high reversibility of the electrochemical process, under these conditions. An explanation for this could be, again, the very low potential scan rate by which these curves are recorded. Peak R2 appears after the oxidation of the redox couple and maintains a somewhat higher variation than the first, in accordance with what is also observed in CV (Figure 2a). Starting at pH 3.8, however, the peak begins to move with a greater slope, also coinciding with its disappearance, so this measurement could be unrealistic.

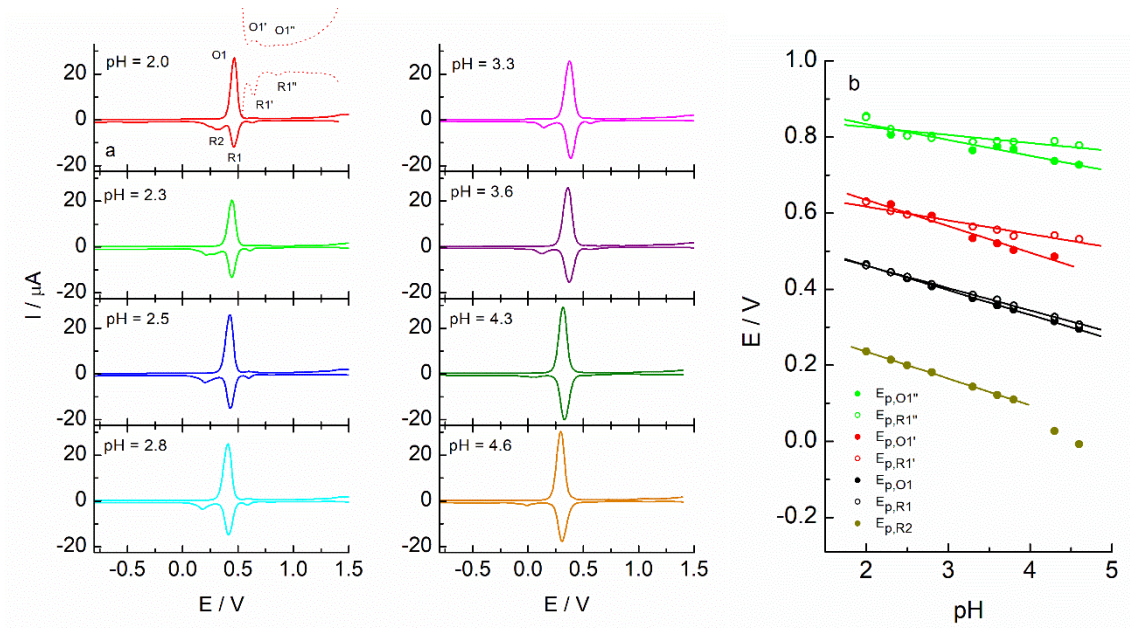


Figure 3. a) DPVs of pPD 1 mM in 0.1 M Britton-Robinson buffer at different pH. Insert: a magnification in intensity for part of the DPV at pH 2.0 is shown (red dotted line) to highlight the peaks mentioned in the text. b) Variation of E_p vs. pH.

Table 2. Experimental variations of E_p vs. pH for the oxidation and reduction peaks of the redox processes of pPD in aqueous solutions obtained by DPV.

Peak	pH interval	$\partial E_p / \partial \text{pH}$ (Ox)	$\partial E_p / \partial \text{pH}$ (Red)
O1''/R1''	2 < pH < 5	-42.0	-21.0
O1'/R1'	2 < pH < 5	-69.2	-36.0
O1/R1	2 < pH < 5	-64.9	-58.6
R2	2 < pH < 3.8	--	-70.5

3.2.2. Influence of the scan rate in CV

To investigate the electrochemical process, the effect of the scan rate was studied. Firstly, pH 1.8 conditions have been chosen as representative of the acid medium interval, which is where the R2 peak appears. This pH value is the lowest reached with the Britton-Robinson buffer used in this work. However, to see if the observed behavior continues under more acidic conditions, cyclic voltammograms have been taken in HCl and H₂SO₄ media. Although at pH 1, the signals are similar to that at pH 1.8, lowering the pH further, the process get more complex as it is observed in Figure S2.

For the analysis of the peak currents, Randles-Sevcik equations for reversible and irreversible cases (equations 1 and 2, respectively) [34, 35] can be used to get an initial idea of the electrochemical process [36, 37],

$$j_p = 0.446nFA[C]_o(nFDv/RT)^{1/2} \quad (1)$$

$$j_p = 0.496n\sqrt{n' + \beta_{n'+1}}FA[C]_o(FDv/RT)^{1/2} \quad (2)$$

where j_p are the peak current, n is the overall number of electrons transferred, n' is the number of electrons prior to the rate determining step, $\beta_{n'+1}$ is the electron transfer coefficient of that step, F is the Faraday constant, C_o is the concentration, A is the electrode area, v is the scan rate, D is the diffusion coefficient, R is the gas constant, and T is the absolute temperature.

Figure 4a shows the comparison between the Randles-Sevcik theoretical predictions for three different mechanisms, a two-electron oxidation with and without a prior electron being transferred before the rate determining step, and a single two step involving two electrons. To obtain these plots, a diffusion coefficient of $8.2 \times 10^{-6} \text{ cm}^2/\text{s}$ has been used that corresponds to the average of values obtained by chronoamperometry and rotating disk electrode voltammetry (see below). The experimental results are also plotted, indicating that the best fit for the data is the single step involving two electrons, at least at low scan rates. The obtained slope ($1.52 \times 10^{-4} \text{ A} \cdot \text{V}^{-1/2} \cdot \text{s}^{1/2}$) agrees with the involvement of two electrons and a diffusion coefficient of $8.2 \times 10^{-6} \text{ cm}^2/\text{s}$, a value that is similar to reported literature values [21].

Figure 4b presents a set of normalized voltammograms at different scan rates. For normalization, equation (1) has been used, following the operation $\psi = \frac{j_p}{0.446FA[C]_o(FDv/RT)^{1/2}} = n^{3/2}$, so that the height of the peak will be related to the number of electrons involved in the process ($n \sim 2$, in the present case) and can report on the rate-determining step, in the case the system is not reversible.

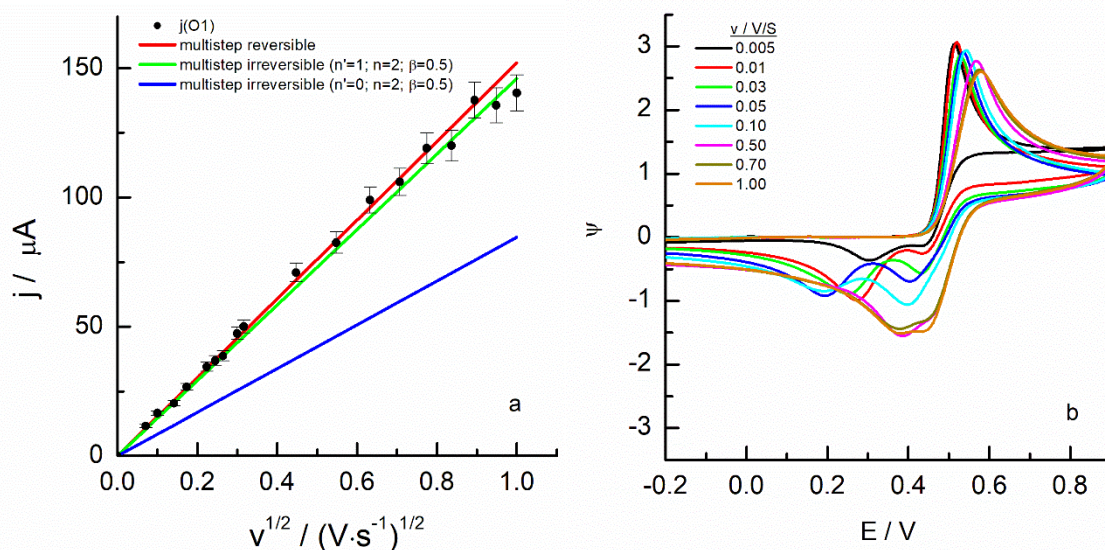


Figure 4. (a) Plot of the pPD oxidation peak current (error bars correspond to the average of three independent measurements) as a function of the square root of the scan rates, compared to the theoretical plots of Randles-Sevcik equations, as indicated in the text. (b) CVs of pPD 1 mM in 0.1

M Britton-Robinson buffer at pH 1.8. The CVs have been normalized according to eqn. 1, as indicated in the text.

The voltammogram recorded at low scan rate shows an oxidation peak at 0.515 V and two reduction peaks at $E_p(R1) = 0.430$ V and $E_p(R2) = 0.300$ V. The normalized oxidation current decreases moderately (around 15%), from a value of approximately 3 at low scan rates, to 2.6 at the highest scan rate studied. These values give an approximate value of $n = 2$, according to equation 1. Meanwhile, the cathodic peaks show a more complex behavior. Thus, the R1 peak begins with very low intensity and strongly shifts to lower potentials, with a relative increase in current up to $v > 0.5$ V/s, from where it remains practically constant. The R2 peak also shifts towards less positive values, maintaining a separation with R1 that reaches the value of 200 mV, disappearing or mixing with R1 from 0.5 V/s. Thus, the current ratio of the two cathodic peaks, j_{R1}/j_{R2} , increases with the scan rate until the R2 peak disappears, and from there, the voltammogram shows the characteristics of an apparent quasi-reversible two-electron process. This behavior would indicate that the electrochemical oxidation of pPD is accompanied by a rapid chemical reaction. Hence, when the scan rate is very slow, there is time for the signal to be affected, showing this fact as a decrease in j_{R1} and the appearance of R2. At higher speeds, there is an overlap of the two peaks, and it is not possible to discriminate between the two signals. With this consideration, R1 must correspond to the reduction of the oxidation product generated in the direct scan (O1 peak), whereas R2 should be the reduction of the product of the subsequent chemical reaction.

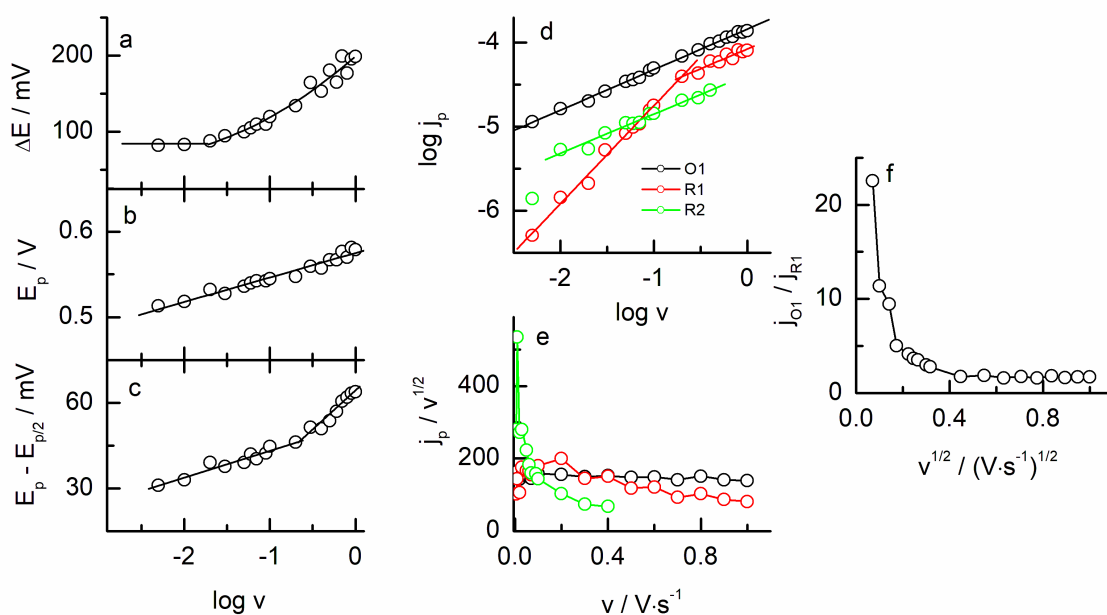


Figure 5. Analysis of the CV parameters corresponding of the voltammograms of Figure 4b. Variation of the potential peak separations ($E(O1) - E(R1)$, ΔE) (a), potential peak (E_p) (b), peak half-width ($E_p - E_{p/2}$) (c) against the logarithm of the scan rate. Logarithmic variation of the current intensity (d) and current function (e) for the three main electrochemical signals (as indicated in the figure label). Variation of the current ratio j_{O1}/j_{R1} (f) as a function of the square root of the scan rate.

The peak potential separation (ΔE) is of 80 mV at low scan rates and increases up to 200 mV at higher scan rates (Figure 5a). Considering that the redox process involves two electrons, these values would indicate that the system shows a certain degree of reversibility. The rate constant for the electrochemical reaction, as determined by the Nicholson method [38], gives a value of $k^0 = 6 \times 10^{-4}$ cm/s. As the scan rate increases, the anodic peak shifts to more positive potentials ($\partial E_p / \partial \log v = 28$ mV/dec) (Figure 5b), according to equation (3) [34], that predicts potential shifts to higher values and is derived for electrode processes followed for an irreversible first-order chemical reaction.

$$\frac{\partial E_p}{\partial \log v} = \frac{2.303RT}{2F} = 30 \text{ mV} \quad (3)$$

It can be observed in the voltammograms that the half-width of the oxidation peak increases slightly with the scan rate and, as shown in Figure 5c, a drastic change in the $E_p - E_{p/2}$ parameter occurs at values higher than 0.3 V/s. For a reversible process, the value of this parameter is given by equation (4) [34]:

$$|E_p - E_{p/2}| = 2.218 \frac{RT}{nF} = \frac{47}{n} \text{ mV a } 298^\circ \text{C} \quad (4)$$

Thus, the theoretical value of 23.5 mV predicted for a two-electron process is somewhat lower than the 30 mV obtained at low rates. Furthermore, this value increases until it reaches 60 mV, which would imply that the process is in some way influenced either by the values of the formal potentials of the two individual electron transfer reactions (E_2^0 y E_1^0) [39] or by the rate constants of these electron transfers.

As shown in Figure 5d, the logarithmic plots of the current intensity present slopes close to 0.5, except for R1 at low values, which shows a slope around unity. Although this value is indicative of an adsorption process, this is actually apparent, and would account for the evolution of the chemical reaction that prevents the reduction of the oxidized form, up to it changes to diffusion control, when the scan rate increases. In this way, the system can be treated, in general, as diffusion controlled, in particular, regarding the oxidation peak which, as seen in Figure 4a, shows a linear variation with the square root of the scan rate (following eqn. 1). In Figure 5e, the current function has been represented in the form $j_p/v^{1/2}$ for the three signals, finding that both the O1 and the R1 peak current functions ($\sim 150 \mu\text{A}(\text{V}\cdot\text{s}^{-1})^{-1/2}$) are practically constant, as it is

typical of the reversible processes [40]. However, the function for R2 starts with a high value ($> 400 \mu\text{A}(\text{V}\cdot\text{s}^{-1})^{-1/2}$) and sharply decreases until it reaches an almost constant value before the peak disappears. The value of $j_{\text{O}1}/j_{\text{R}1}$ is very high at low scan rate and drops drastically with increasing this variable, remaining practically constant and somewhat greater than unity at $v > 0.4 \text{ V/s}$ (Figure 5f). These results are both in agreement with the presence of a chemical reaction preceding peak R2, that is manifested at low scan rates as discussed above.

It has been described that the oxidation product of pPD is the corresponding quinone diimine (pPDI) as stated in reactions (i) to (iii) and Scheme 2 and that, it can suffer a hydrolysis reaction in one of the imine groups that would give rise to the corresponding quinone monoimine. Under these conditions, the quinone monoimine could be reduced at the potentials corresponding to R2 [41]. A proof that this can be the case is obtained by carrying out a second consecutive scan in which a second oxidation signal, O2, appears prior to the main oxidation peak and which should be due to the product obtained in R2 (Figure S3 and S4). It is interesting to note that the O2 peak only appears at low scan rate, disappearing in parallel with the R2 peak. It has recently been described that a sulfonamide derivative with a base structure of pPD shows a similar behavior in acidic medium. The authors ascribe the signal to the presence of a chemical reaction that transforms the oxidation product into an electroactive species [42]. They conclude that the chemical reaction is a dimerization. However, in our case, the dependence of the current density with the pPD concentration shows a first order behavior (Figure S5), which indicates that a dimerization reaction does not occur.

Thus, the presence of the second reduction peak R2 points to the existence of a subsequent chemical reaction that gives rise to an electroactive species that is reduced in that peak. As demonstrated in Figure S3, this reaction is first order, so it is assumed that it is the hydrolysis reaction of pPDI^+ that should occur easily in an acidic medium [8].

3.2.3. Rotating Disk Electrode voltammetry.

To complement the study, the electrochemical response of pPD has been analyzed using a rotating GC electrode (RDE), at different rotation speeds (ω), with a scan rate of 5 mV/s. The curves show the normal behavior, showing a rise in intensity as ω increases. These voltammograms are characterized by the mass transport limiting current parameters, j_L , and by the half-wave potential, $E_{1/2}$, which corresponds to the point at which the current is $j = j_L/2$. Figure 6 shows the curves obtained at ω between 2.5 and 314.2 s^{-1} along with the variations of j_L and $E_{1/2}$. For this analysis, the Levich equation (equation 5) is used, which relates the limiting current to the square root of ω :

$$i_L = 0.62nFAD^{2/3}\nu^{-1/6}C\omega^{1/2} \quad (5)$$

where n is the number of electrons transferred, A is the electrode area, ν is the kinematic viscosity of the solution and the rest of the parameters have their usual meaning. As can be seen, the plot of j_L vs $\omega^{1/2}$ is linear in a wide range of rotation speeds ($\omega < 150 \text{ s}^{-1}$). From the slope of this graph (6.2×10^{-6}) and taking into account that the number of electrons involved in the process is 2, a diffusion coefficient of $6.9 \times 10^{-6} \text{ cm}^2 \text{ s}^{-1}$ is determined, very close to that obtained using CV. On the other hand, the $E_{1/2}$ values vary linearly with the $\log \omega$ ($\omega < 100 \text{ s}^{-1}$), giving a slope of 23 mV/dec. At higher rotation speeds the magnitude of the displacement of the curves becomes much greater, indicating an increase in the irreversibility of the process.

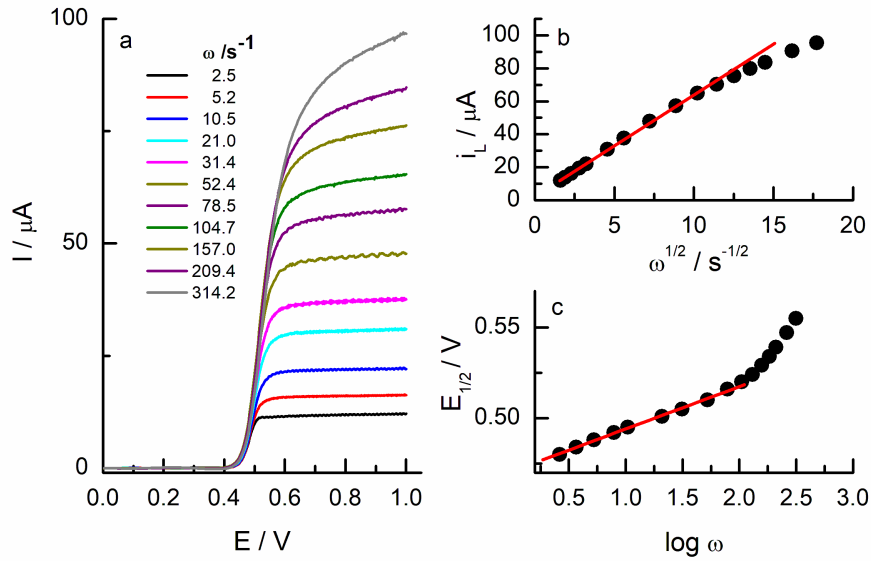


Figure 6. (a) RDE voltammograms of pPD 1 mM in Britton – Robinson buffer 0.1 M at pH 1.8. (b) Levich plot and (c) $E_{1/2}$ vs $\log \omega$ for the data measured in the RDE voltammograms.

The Levich equation predicts the ideal response of fast electron transfer processes. A deviation in a Levich representation from a line intercepted at the origin therefore suggests that there is a kinetic limitation on the electron transfer reaction [43]. For processes with slow electron transfer, the system shows a mixed kinetic – mass transport control and the Koutecky – Levich treatment (equation 6) predicts the proportionality between the inverses of j_L vs $\omega^{1/2}$, according to the equation:

$$\frac{1}{j_L} = \frac{1}{j_k} + \frac{1}{j_D} = \frac{1}{nFAk_hC} + \frac{1}{0.62nFAD^{2/3}\nu^{-1/6}C\omega^{1/2}} \quad (6)$$

where k_h is the heterogeneous electron transfer rate constant, j_k represents the kinetic current in the absence of diffusion limitation and j_D the diffusion current. The Koutecky – Levich

representations made at various potentials within the range of the signal are linear, indicating that oxidation is controlled by diffusion. In the present case, the intercepts are a function of the potential, while the slopes depend on this variable, at low overpotentials, and end up becoming independent at high values, that is, when $E > E_{1/2}$.

In the case of multielectron mechanisms, such as the one that takes place for pPD, it has been described that, when both the intercepts and the slopes of the Koutecky – Levich plots depend on the potential, one of the steps of electron transfer is irreversible and the slope is proportional to the total number of electrons involved in the process, that is, the sum of the electrons that participate in the fast steps plus that of the rate-determining step. Therefore, this number will be less than or equal to the total number of electrons obtained by chronoamperometry or exhaustive electrolysis [44]. Under these conditions, the number of electrons involved in the process can be determined, which turns out to be of 2.1, in agreement with the above results obtained by electrolysis and chronoamperometry.

The intercept corresponds to the kinetic current in the absence of diffusion limitation. From the kinetic currents determined in the representations, the values of k_h are obtained as a function of the applied overpotential. Under these conditions, the Butler–Volmer equation can be used to calculate the intrinsic rate constant k_o , from equation 7:

$$k_o = \frac{k_h}{\exp\left(\frac{\beta n F (E - E_{1/2})}{RT}\right)} \quad (7)$$

Figure 7 shows the representation of $\ln k_h$ versus the overpotential, showing linearity in an important range of overpotentials. A k_o value of 6.4×10^{-4} cm/s, in agreement with CV, and an apparent value of 2 electrons involved in the process are obtained.

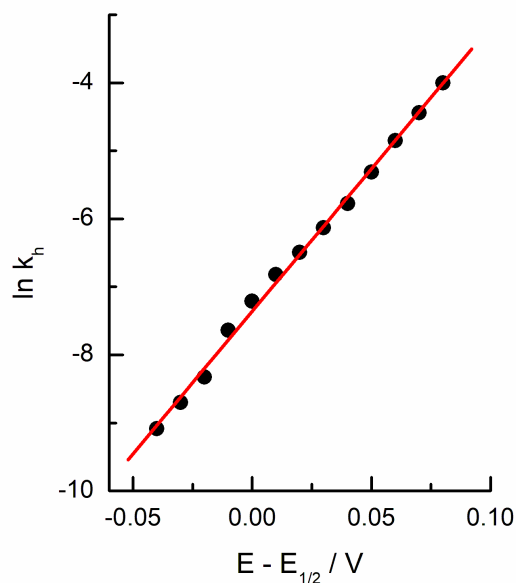


Figure 7. Plot of $\ln k_h$ vs. overpotential, determined from the results obtained by representing the Koutecky – Levich equation at different overpotentials. (pPD) = 1 mM, Britton – Robinson buffer 0.1 M. pH 1.8.

3.2.4. Tafel analysis

To get more insight into the oxidation mechanism of pPD, Tafel analysis has been carried out as a function of both the scan rate and the rotation speed. The equation 8 that gives the values of $n' + \beta_{n'+1}$ as slopes has been used (these parameters have the same meaning as before) [45].

$$\frac{RT}{F} \frac{\partial \ln j}{\partial E} = (n' + \beta_{n'+1}) \quad (8)$$

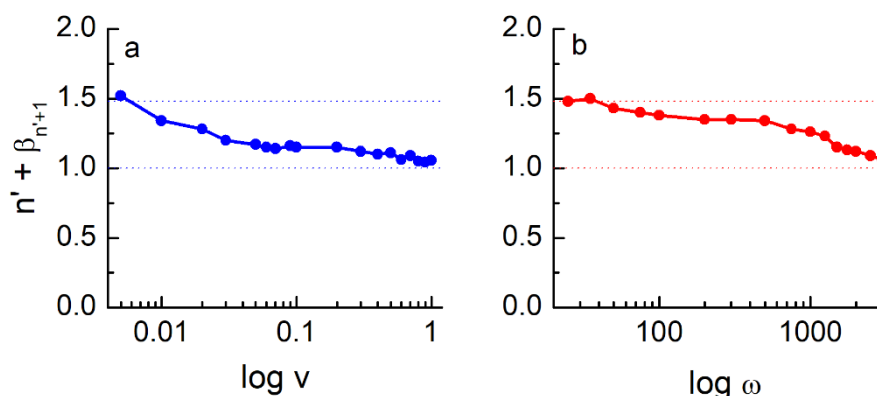


Figure 8. Variation of the Tafel parameter $n' + \beta_{n'+1}$ as a function of the scan rate (a) and rotation speed (b). (pPD) = 1 mM, 0.1 M Britton-Robinson buffer, pH 1.8.

The values obtained are plotted in Figure 8 and, in both cases, vary from a value of approximately 1.5 at lower scan rates or rotation speeds to 1 at the highest values studied. It is interesting to note that both techniques give the same behavior. Two regimes are distinguished that can be represented by the transfer of two electrons, being the second slower than the first one (EEi) at low values followed by an ECiE mechanism at the higher rates [35, 46].

From these results, an oxidation mechanism can be established for pPD in the acid region that, in general, follows the quasi-reversible two-electron reduction. As shown in Scheme 2 [17], starting from the species in solution at $\text{pH} < 2.8$, pPDH_2^{2+} , it must lose a proton to give the electroactive species, pPDH^+ . The loss of this H^+ ion is gently observed in the variation of E_p with pH in this region (Figure 2), which presents a value of -82.4 mV/pH . However, the release of this proton must be rapid since it is not detected in the DPVs, in which the curves are registered at a much lower scan rate. Furthermore, in the study as a function of the scan rate, it is observed that the current function for the oxidation peak shows a constant value (Figure 5e), which indicates the absence of a previous chemical reaction to electron transfer. On the other hand, the presence of a single oxidation peak together with the value of the normalized current (Figure 4b) indicate that the peak involves the transfer of 2 electrons, which is in agreement with the RDE study.

Therefore, the first electron transfer will give rise to the species pSQH_2^{2+} which, having an acid dissociation constant of around 0.7 (determined through a thermodynamic cycle [17]), must be promptly transformed to pSQH^+ which must be instantly oxidized since its oxidation potential practically coincides with the values at which the species is generated. Again, under these conditions, the pPDIH_2^{2+} species that is generated must rapidly transform into pPDIH^+ , which is the stable species in solution, as deduced from its pK value [8, 17].

At this point, it is interesting to note that when the scan rate increases, the Tafel slope decreases to the unity ($n' + \beta_{n'+1} = 1$), that means that the rate determining step must be a chemical reaction and the number of electrons transferred before this step is the unity. Thus, under these conditions, an EC_iE mechanism can be contemplated involving the reaction of the free radical pSQH_2^{2+} releasing the H^+ ion as rate determining step (Scheme 2).

3.2.5. Controlled potential electrolysis.

To complete the picture and get more insight into the fate of the oxidation products of pPD and the subsequent chemical reaction evidenced by the reduction peak R2 in the voltammograms, a study of controlled potential electrolysis at $\text{pH} 1.8$ has been carried out. The

course of the controlled potential electrolysis has been followed by CV and UV-visible absorption spectroscopy. Figures 9 and 10 show the voltammograms and spectra recorded for pPD at the beginning of the electrolysis, and these at the different electrolysis times.

As can be seen at short electrolysis times, the voltammograms show decreases in the O1 and R1 peaks, in parallel with an increase in the R2 peak. Furthermore, a small shoulder is observed at potentials less positive than the O1 peak that coincides with the one that appears in the second cycle recorded with pPD (see Figures S3 and S4). This fact would indicate that the oxidized species ($\text{pPDIH}_2^{2+}/\text{pPDIH}^+$) rapidly suffers a chemical transformation to an electroactive species that is stable and remains in the electrolysis mixture. As the electrolysis time increases, the R1 peak continues decreasing, concomitant with the increase of R2 and the development of O2, as O1 disappears. After approximately 30 min, the charge exchanged in the electrolysis begins to increase very slowly and the voltammetric signals show a certain constancy, so it is concluded that the electrolysis is not progressing and should be considered as terminated.

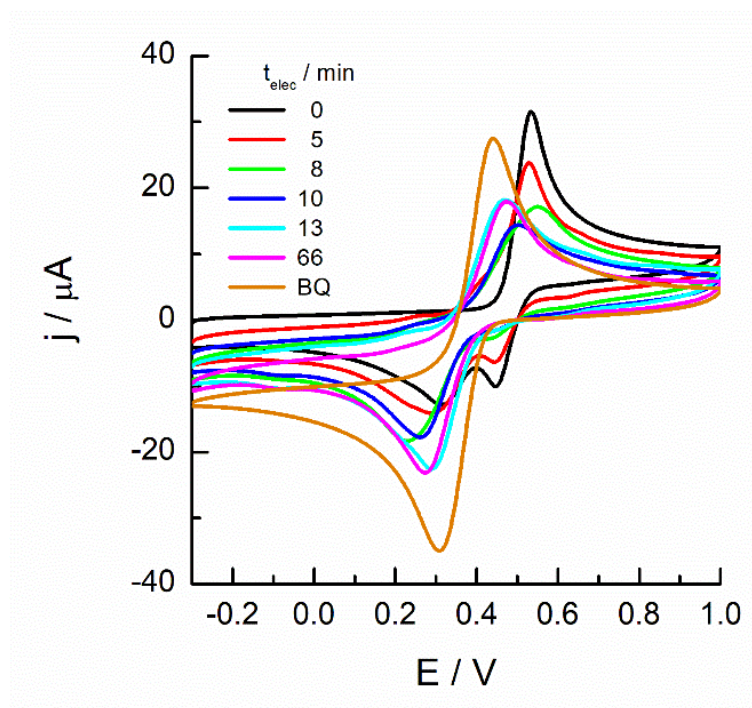


Figure 9. Monitoring the course of the controlled potential electrolysis at 1 V of 5mM pPD in 0.1 M Britton – Robinson buffer at pH 1.8, using CV. Cyclic voltammograms recorded at different electrolysis times, after diluting an aliquot in the corresponding buffer to get 1 mM pPD. $v = 0.05$ V/s. The orange curve corresponds to a spectrum taken from a 1 mM BQ solution under the same experimental conditions.

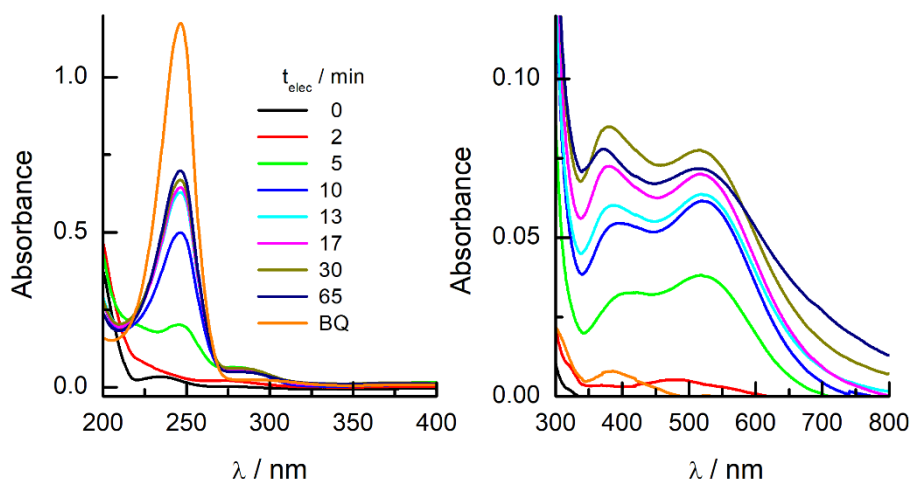


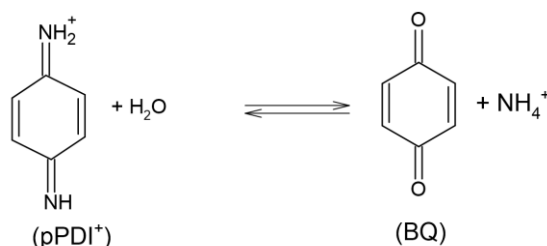
Figure 10. Monitoring the course of the controlled potential electrolysis at 1 V of 5mM pPD in 0.1 M Britton – Robinson buffer at pH 1.8, using UV-visible absorption spectroscopy. The spectra were recorded at different electrolysis times, after diluting an aliquot in the corresponding buffer to get 1 mM pPD. Optical pathlength: (left) 0.2 cm; (right) 1 cm. The orange curve corresponds to a spectrum taken from a 1 mM BQ solution under the same experimental conditions.

The UV-visible spectra also show a similar trend. The pPD spectrum under these pH conditions shows two bands at 232 and 284 nm that, as the electrolysis progresses, transforms into a main band at 245 nm that develops until it becomes invariant. At the same time, two bands appear at higher wavelengths (380 and 530 nm) that must be responsible for the strong color changes of the solution. These bands, however, are of very low intensity, compared to the signal at 245 nm.

The total charge passing through the whole process together with the analysis of the partial charge measured at different times against the absorbance variations, allows us to determine the number of electrons involved, that results around 2. This contrast with the reported value of 3 determined in the electrolysis carried out at pH 2.2 for the pPD derivative N,N-dimethyl-p-phenylenediamine [14]. To corroborate this data, chronoamperometric experiments have been conducted under similar conditions and the data have been fitted to the Cottrell equation. The curves have been registered at different final potentials within the interval from 0.7 to 1 V and, in all the cases, values of around 2 have been obtained (Figure S6). Thus, we can conclude that the proposed reactions (i), (ii) and Scheme 2 involving 2 electrons and 2 H⁺ ions are operative under these conditions and, the electrolysis leads to the pPDH₂²⁺ / pPDH⁺ species, taking into account the solution pH. However, the observed behavior of the electrolysis reaction mixture points to a subsequent homogenous fast reaction that could indicate a hydrolysis reaction. As this reaction is not a dimerization (section 3.3.2. and Figure S5), it has

been checked if the hydrolysis of one or two imine groups of the pPDIH_2^{2+} / pPDIH^+ species can account for the observed changes. Figure S3 shows the voltammograms of pPD, 4-aminophenol (AP) and benzoquinone (BQ) under the same experimental conditions. AP signal almost coincides with the pPD one and, the anodic new peak observed in the second scan coincides with the BQ peak.

In view of that, the voltammogram and the corresponding absorption spectrum have been recorded for a solution of 1 mM benzoquinone (BQ) under the same experimental conditions. As can be seen in Figure 9, the voltammogram of BQ coincides in shape and potentials with the final electrolysis product and the same can be said for the BQ spectrum (Figure 10). This coincidence, monitored by two different techniques, allows us to conclude that the electroactive species obtained in the electrolysis of pPD, under these pH conditions, is BQ. Therefore, the aforementioned hypothesis of the hydrolysis of pPDI is demonstrated and, furthermore, the main subsequent reaction is the hydrolysis of the two imino groups of the molecule (Scheme 3) [4, 8, 47], instead of that of a single group as has been also mentioned in the literature [20]. With the results obtained, an estimate for the extent of this hydrolysis reaction can be made as a 60%. Thus, the rest of the material could follow other minor reactions as it has also been described [16] and that could lead to the formation of di- and trimeric adducts of the pPD and pPDI molecules, as the Bandrowski base that absorbs at around 550 nm [9]. Moreover, the semiquinone free radical $\text{pSQH}^{\cdot+}$ (Scheme 2) cannot be discarded as it has been reported that it shows absorption at 510 – 550 nm and it can be formed by a combination of pPD and pPDI giving 2 molecules of $\text{pPSQH}^{\cdot+}$, that are fairly stable in solution [48].



Scheme 3. Hydrolysis reaction of pPDI^+ to BQ.

Finally, from these results and taking into account the final products after controlled potential electrolysis, it can be established that the oxidation mechanism of pPD in the acidic range would be described by the route indicated in Scheme 2 (broken orange line) that would continue with the hydrolysis reaction of pPDIH^+ to give the corresponding quinone (Scheme 3)

that undergoes a redox process at potentials somewhat lower than that of the main peak, as it has been shown in Figure S3, S4 and 6.

4. Conclusions.

The electrochemical oxidation of pPD in aqueous solutions follows a general two-electron oxidation process that is somewhat dependent on the solution pH. This dependence is strongly related to the acid-base dissociation equilibria of the molecule and, most importantly, to those of the intermediates and final reaction products. Even though the oxidation mechanism is simple, there is a high complexity in the global process, as many different subsequent homogeneous reactions can take place involving not only the final redox products but also, the parent diamine molecule and the intermediates.

In acidic solutions, the oxidation is a $2e$, $3H^+$ or $2H^+$ reaction but the voltammetry is complicated by the presence of a second reduction peak whose intensity is strongly dependent on the scan rate and the solution pH. This second peak is only clearly observed at low scan rates under the experimental conditions of the present study. This means that the reaction needs a time interval of few seconds to be observed. The controlled potential electrolysis helps in the understanding of this process that takes place in parallel with the main oxidation reaction and points to the hydrolysis reaction of the two imine groups of the quinone diimine oxidation product.

The presence of this reaction complicates the redox mechanism that shows a quasi-reversible behavior with a first reversible electron transfer step followed by a quasi-reversible second one. Although this EE mechanism should involve an intermediate chemical step, it is not observed at low scan rates and/or low rotation speed, as reflected in the Tafel slope values. However, at higher values of these parameters, the mechanism is transformed in an ECE, that should account for the finite time that would take the intermediate chemical reaction.

Acknowledgements. We thank the Ministerio de Ciencia e Innovación (Project RED2022-134120-T Network of Excellence Electrochemical Sensors and Biosensors), Junta de Andalucía and Universidad de Córdoba for financial support of this work. A. F. M. acknowledges Ministerio de Universidades (FPU 17/02616); R. d C. acknowledges Consejería de Universidades, Junta de Andalucía (POSDOC_21_00033).

6. Bibliography

- [1] L. He, F. Michailidou, H.L. Gahlon, W. Zeng, Hair Dye Ingredients and Potential Health Risks from Exposure to Hair Dyeing, *Chem. Res. Toxicol.* 35(6) (2022) 901-915.
- [2] L.F. Fieser, The Potentials of some Unstable Oxidation-Reduction Systems, *J. Am. Chem. Soc.* 52(12) (1930) 4915-4940.
- [3] L. Michaelis, Semiquinones, the Intermediate Steps of Reversible Organic Oxidation-Reduction, *Chem. Rev.* 16(2) (1935) 243-286.
- [4] L.K.J. Tong, Kinetics of Deamination of Oxidized N,N-Disubstituted p-Phenylenediamines, *J. Phys. Chem.* 58(12) (1954) 1090-1097.
- [5] R.E. Parker, R.N. Adams, Voltammetry at Solid Electrodes, *Anal. Chem.* 28(5) (1956) 828-832.
- [6] L.H. Piette, P. Ludwig, R.N. Adams, Electron Paramagnetic Resonance and Electrochemistry. Studies of Electrochemically Generated Radical Ions in Aqueous Solution, *Anal. Chem.* 34(8) (1962) 916-921.
- [7] H.Y. Lee, R.N. Adams, Anodic Voltammetry and EPR Studies of Isomeric Phenylenediamines, *Anal. Chem.* 34(12) (1962) 1587-1590.
- [8] J.F. Corbett, Benzoquinone Imines. 2. Hydrolysis of p-Benzoquinone monimine and p-Benzoquinone diimine., *J. Chem. Soc. B* (3) (1969) 213-216.
- [9] J.F. Corbett, Benzoquinone Imines. 4. Mechanism and Kinetics of Formation of Bandrowski base, *J. Chem. Soc. B* (7) (1969) 818-822.
- [10] P.J. Elving, A.F. Krivis, Voltammetric Studies with Graphite Indicating Electrode, *Analytical Chemistry* 30(10) (1958) 1645-1648.
- [11] J. Li, X. Gong, The Emerging Development of Multicolor Carbon Dots, *Small* 18(51) (2022) 2205099.
- [12] S. Ramírez-Barroso, A. Jacobo-Martín, I. Navarro-Baena, J.J. Hernández, C. Navio, I. Rodríguez, R. Wannemacher, On the nature of solvothermally synthesized carbon nanodots, *J. Mater. Chem. C* 9(47) (2021) 16935-16944.
- [13] D. Lelievre, A. Henriët, V. Plichon, Electrochemical Oxidation of N,N-Dimethyl-p-Phenylenediamine in Weak Acid-Solution. 1. Thin-Layer Electrochemistry., *J. Electroanal. Chem.* 78(2) (1977) 281-300.
- [14] D. Lelievre, V. Plichon, M.A. Dosal, Electrochemical Oxidation of N,N-Dimethyl-p-Phenylenediamine in Weak Acid-Solution. 2. Electrolysis, *J. Electroanal. Chem.* 78(2) (1977) 301-306.
- [15] C.E. Banks, N.S. Lawrence, R.G. Compton, Sonovoltammetric Elucidation of Electron Transfer Rates: The Oxidation of Dimethyl-p-phenylenediamine in Aqueous Solution, *Electroanalysis* 15(4) (2003) 243-248.
- [16] A.D. Modestov, J. Gun, I. Savotina, O. Lev, On-line electrochemical-mass spectrometry study of the mechanism of oxidation of N,N-dimethyl-p-phenylenediamine in aqueous electrolytes, *J. Electroanal. Chem.* 565(1) (2004) 7-19.
- [17] L.A. Clare, L.E. Rojas-Sligh, S.M. Maciejewski, K. Kangas, J.E. Woods, L.J. Deiner, A. Cooksy, D.K. Smith, The Effect of H-Bonding and Proton Transfer on the Voltammetry of 2,3,5,6-

- Tetramethyl-p-phenylenediamine in Acetonitrile. An Unexpectedly Complex Mechanism for a Simple Redox Couple, *J. Phys. Chem. C* 114(19) (2010) 8938-8949.
- [18] O.V. Klymenko, D. Giovanelli, N.S. Lawrence, N.V. Rees, L. Jiang, T.G.J. Jones, R.G. Compton, The Electrochemical Oxidation of N,N-Diethyl-p-Phenylenediamine in DMF and Analytical Applications. Part I: Mechanistic Study, *Electroanalysis* 15(11) (2003) 949-960.
- [19] V. Solís, T. Iwasita, M.C. Giordano, Para-phenylenediamine oxidation at a platinum electrode in acetonitrile solutions, *J. Electroanal. Chem.* 73(1) (1976) 91-104.
- [20] W.J. Albery, R.G. Compton, I.S. Kerr, The Anodic-Oxidation of 1,4-Diaminobenzene - An Electron-Spin Resonance and Electrochemical Study, *J. Chem. Soc.-Perkin Trans. 2* (5) (1981) 825-829.
- [21] R.G. Compton, P.M. King, C.A. Reynolds, W.G. Richards, A.M. Waller, The Oxidation Potential of 1,4-Diaminobenzene - Calculation versus Experiment, *J. Electroanal. Chem.* 258(1) (1989) 79-88.
- [22] R. Evans, O. Klymenko, C. Hardacre, K. Seddon, R. Compton, Oxidation of N, N, N', N'-tetraalkyl-para-phenylenediamines in a series of room temperature ionic liquids incorporating the bis(trifluoromethylsulfonyl)imide anion., *J. Electroanal. Chem.*, 2003, pp. 179-188.
- [23] R. Evans, O. Klymenko, P. Price, S. Davies, C. Hardacre, R. Compton, A comparative electrochemical study of diffusion in room temperature ionic liquid solvents versus acetonitrile., *ChemPhysChem*, 2005, pp. 526-533.
- [24] J. Long, D. Silvester, A. Barnes, N. Rees, L. Aldous, C. Hardacre, R. Compton, Oxidation of several p-phenylenediamines in room temperature ionic liquids:: Estimation of transport and electrode kinetic parameters, *J. Phys. Chem. C*, 2008, pp. 6993-7000.
- [25] E. Barnes, A. O'Mahony, S. Belding, R. Compton, Kinetics and Thermodynamics of Redox Processes in Room Temperature Ionic Liquids: The Use of Voltammetry and the Disproportionation of Radical Cations of N, N-Dimethyl-p-phenylenediamine in 1-Butyl-3-methylimidazolium Tetrafluoroborate], *J. Chem. Engineering Data*, 2010, pp. 2219-2224.
- [26] F. Cataldo, On the polymerization of P-phenylenediamine, *Eur. Polymer J.* 32(1) (1996) 43-50.
- [27] X.-G. Li, M.-R. Huang, W. Duan, Y.-L. Yang, Novel Multifunctional Polymers from Aromatic Diamines by Oxidative Polymerizations, *Chem. Rev.* 102(9) (2002) 2925-3030.
- [28] B. Lakard, G. Herlem, S. Lakard, B. Fahys, Ab initio study of the polymerization mechanism of poly(p-phenylenediamine), *J. Mol. Structure: THEOCHEM* 638(1) (2003) 177-187.
- [29] Y.-Q. Dai, D.-M. Zhou, K.-K. Shiu, Permeability and permselectivity of polyphenylenediamine films synthesized at a palladium disk electrode, *Electrochim. Acta* 52(1) (2006) 297-303.
- [30] R.H. Sestrem, D.C. Ferreira, R. Landers, M.L.A. Temperini, G.M. do Nascimento, Structure of chemically prepared poly-(para-phenylenediamine) investigated by spectroscopic techniques, *Polymer* 50(25) (2009) 6043-6048.
- [31] S.M. Sayyah, S.S. Abd El-Rehim, M.M. El-Deeb, S.M. Kamal, R.E. Azooz, Electropolymerization of p-phenylenediamine on Pt-electrode from aqueous acidic solution: Kinetics, mechanism, electrochemical studies, and characterization of the polymer obtained, *J. Appl. Polymer Sci.* 117(2) (2010) 943-952.
- [32] J.F. Corbett, Benzoquinone Imines. 1. p-Phenylenediamine-Ferricyanide and p-Aminophenol-Ferricyanide Systems, *J. Chem. Soc. B* (3) (1969) 207-212.

- [33] G. Moro, A. Silvestri, A. Ulrici, F. Conzuelo, C. Zanardi, How to optimize the analytical performance of differential pulse voltammetry: one variable at time versus Design of Experiments, *J. Solid State Electrochem.* 28(3) (2024) 1403-1415.
- [34] R.G. Compton, C.E. Banks, *Understanding voltammetry*, World Scientific 2018.
- [35] C. Batchelor-McAuley, R.G. Compton, Voltammetry of multi-electron electrode processes of organic species, *J. Electroanal. Chem.* 669 (2012) 73-81.
- [36] R.P. Bacil, L. Chen, S.H.P. Serrano, R.G. Compton, Dopamine oxidation at gold electrodes: mechanism and kinetics near neutral pH, *Phys. Chem. Chem. Phys.* 22(2) (2020) 607-614.
- [37] R.P. Bacil, P.H.M. Garcia, S.H.P. Serrano, New insights on the electrochemical mechanism of epinephrine on glassy carbon electrode, *J. Electroanal. Chem.* 908 (2022) 116111.
- [38] R.S. Nicholson, Theory and Application of Cyclic Voltammetry for Measurement of Electrode Reaction Kinetics, *Anal. Chem.* 37(11) (1965) 1351-1355.
- [39] R.L. Myers, I. Shain, Determination of E20 - E10, for overlapping waves in stationary electrode polarography, *Anal. Chem.* 41(7) (1969) 980-980.
- [40] R.S. Nicholson, I. Shain, Theory of Stationary Electrode Polarography. Single Scan and Cyclic Methods Applied to Reversible, Irreversible, and Kinetic Systems, *Anal. Chem.* 36(4) (1964) 706-723.
- [41] D. Hawley, R.N. Adams, Homogeneous chemical reactions in electrode processes: Measurement of rates of follow-up chemical reactions, *J. Electroanal. Chem.* 10(5) (1965) 376-386.
- [42] M.R. Talebi, D. Nematollahi, A.R. Massah, Comparative electrochemical study of N-(4-aminophenyl) and N-(4-hydroxyphenyl)benzenesulfonamide derivatives, *Electrochim. Acta* 457 (2023) 142499.
- [43] F. Opekar, P. Beran, Rotating disk electrodes, *J. Electroanal. Chem.* 69(1) (1976) 1-105.
- [44] S. Treimer, A. Tang, D.C. Johnson, A Consideration of the Application of Koutecký-Levich Plots in the Diagnoses of Charge-Transfer Mechanisms at Rotated Disk Electrodes, *Electroanalysis* 14(3) (2002) 165-171.
- [45] R. Guidelli, R.G. Compton, J.M. Feliu, E. Gileadi, J. Lipkowski, W. Schmickler, S. Trasatti, Defining the transfer coefficient in electrochemistry: An assessment (IUPAC Technical Report), 86(2) (2014) 245-258.
- [46] S. Fletcher, Tafel slopes from first principles, *J. Solid State Electrochem.* 13(4) (2009) 537-549.
- [47] A. Maleki, D. Nematollahi, Mechanism diversity in anodic oxidation of N,N-dimethyl-p-phenylenediamine by varying pH, *Journal of Electroanalytical Chemistry* 704 (2013) 75-79.
- [48] U. Nickel, C.V. Peris, U. Ramminger, A Radical Chain Mechanism Coupled to Autocatalysis. The Oxidation of N,N-Dimethyl-p-phenylenediamine by Peroxodisulfate, *J. Phys. Chem. A* 106(15) (2002) 3773-3786.